First principales calculations of structural, Thermodynamic, electronic and optical Properties of $CaS_{1-x}Se_x$ Semiconducting Alloy.

M. Slimani[1], **C.** Sifi[1], **H.** Meradji[1], S.Ghemid[1]

[1] *Loboratory LPR Physics Department, Faculty of Science, University of Annaba. 23000 Annaba,* Algeria.
First-Third Department, First-Third University

menoubas@yahoo.fr

Abstract— The full potential-linearized augmented plane wave (FP-LAPW) method within density functional theory (DFT) was applied to study the structural, electronic, optic and thermodynamic properties of CaS1-xSe$_x$ temary alloys. The local density approximation was used with generalized gradient correction (GGA) as well as the Engel-Vosko GGA formalism to calculate band gap. The effect of composition on lattice constants, bulk modulus and band gap was investigated. Deviation of the lattice constants from Vegard's lawand the bulk modulus from linear concentration dependence (LCD) were observed for the three alloys. The microscopie origins of the gap bowing were explained by using the approach of Zunger and co-workers. In order to investigate the thermodynamic stability of the alloys we first calculated the excess enthalpy of mixing ΔH_m as a function of concentration (x). Then by using a regular model solution the x-dependent interaction parameter, Ω, was obtained from the result of DHm versus x. Finally, by using this Ω value, the phase diagram of the alloys was calculated. It was shown that all of these alloys are stable at high temperature. On the other hand, an accurate calculation of linear optical functions (refraction index and both imaginary and real parts of the dielectric function).

Keywords— FP-LAPW, Band gap, structural and optical properties, Phase diagramme.

I. INTRODUCTION

Semiconductor alloys, which are solid solutions of two or more semiconducting elements, have important technological applications, especially in the manufacture of electronic and electro-optical devices. One of the easiest ways to change artificially the electronic and optical properties of semiconductors is by forming their alloys; it is then interesting to combine two different compounds with different optical band gaps and different rigidities in order to obtain a new material with intermediate properties. Hence, the major goal in materials engineering is the stability to tune the band gap independently in order to obtain the desired properties. The alkaline earth chalcogenides (AX: A = Be, Ca, Mg, Sr, Ba; X = O, S, Se, Te) form a very important closed shell ionic system crystallizing in NaCl-type structure at room conditions except for the MgTe and the beryllium chalcogenides. These compounds are technologically important materials having many applications ranging from catalysis to microelectronics. They have also application in the area of luminescent devices [1-3].

In fact, one of the easiest ways to change artificially the electronic and optical properties of semiconductors is by forming their alloys; It is then interesting to combine two different compounds with different optical band gaps and different rigidities in order to obtain a new material with intermediate properties. Therefore, a great deal of progress has made in the last few decades in understanding the effects of disorder in random alloys. Zunger and co-workers [4] have introduced an approach that greatly reduces the size of the supercell required to obtain a realistic description of a random alloy by using so-called 'special quasirandom structures (SQSs).

In this paper, we model $CaS_{1-x}Se_x$ ternary alloys at some selected compositions with ordered structures described in terms of periodically repeated supercells (SQSs). In order to carry out our calculations, we have applied the full potential-linearized augmented plane wave (FP-LAPW) method. On one hand we focused our efforts on the physical origins and variation of the optical band gap within the alloy fraction; on the other hand we address the more fundamental issue of the phase stability and exploring the optical properties of these alloys.

II. METHOD OF CALCULATIONS

In order to calculate the structural and electronic properties of $CaS_{1-x}Se_x$ alloys, we have employed the FP-LAPW method [5] to solve the kohn-Sham equations. We have performed our calculations by the WIEN2K code [6] within the framework of density functional theory (DFT) [7], that has been shown to yield reliable results for the electronic and structural properties of various solids. The exchange-correlation contribution is described within the generalized gradient approximation (GGA) based on Perdew et al. [8] to calculate the total energy, while for the electronic properties, in addition to the GGA correction the Engel-Vosko (EVGGA) [9] scheme was also applied. In the FP-LAPW approach the wave function, charge density and potential are expanded differently in the two regions ofthe unit cell. Inside the non-overlapping spheres of radius R_{MT} around each atom, spherical harmonic expansions are used, while in the remaining space of the unit cell a plane wave basis set is chosen. The muffin-tin radius R_{MT} were assumed to be 2.2, 2.3, 2.4, and 2.5 au for S, Ca, Se and Te atoms, respectively. A mesh of 47 special k-points for binary compounds and 125 special k-points for alloys were taken in the irreducible wedge of the Brillouin zone for the total energy calculation. The maximum l value for the wave function expansions inside spheres was confined to $l_{max}=10$. The plane wave cut-off of $K_{max}= 8.0/R_{MT}$ is chosen for the expansion of the wave functions in the interstitial region while the charge density was Fourier

expanded up to G_{max} =14 (Ryd)$^{1/2}$. Both the plane wave cut-off and the number of k-points are varied to ensure total energy convergence.

III. RESULTS AND DISCUSSION

A. STRUCTURAL PROPERTIES

In this section, we have analyze the structural properties of CaX (X = S, Se, Te) compounds in the rocksalt structure using the GGA scheme. The alloys have been modeled at some selected compositions (x = 0.25, 0.5, 0.75) following the SQS approach. For the considered structures, we perform the structural optimization by minimizing the total energy with respect to the cell parameters and also the atomics positions.

The total energy calculated as a function of unit cell volume where fitted to the murnaghan's equation of state [10]. The equilibrium lattice constants and bulk modulus both for binary compounds and their alloys are given in table 1. Considering the general trend that GGA usually overestimates the lattice parameters [11], our GGA results of binary compounds are in reasonable agreement with the experimental and other calculated values.

Tableau 1. Calculated lattice parameter (a) and bulk modulus B of CaS, CaSe and CaTe compounds and their alloys at equilibrium volume.

	x	Lattice constant a (A)			Bulk modulus B (GPa)		
		this work	Experimett [17]	other calculation[18]	this work	Experiment [17]	other calculation [18]
CaS$_{1-x}$Se$_x$	1	5.964	5.916	5.829	47.958	51	56.2
	0.75	5.906			49.910		
	0.5	5.847			52.499		
	0.25	5.787			55.176		
	0	5.722	5.689	5.598	57.106	64	65.2

Usually, in the treatment of alloys, it is assumed that the atoms are located at the ideal lattice sites and the lattice constant varies linearly with according to the so-called Vegard's law [12]. However, violation in this linear law has been reported in semiconductor alloys both experimentally [13, 14] and theoretically [15, 16]. As an example the results obtained for the composition dependence of the calculated equilibrium lattice parameter for CaS$_{1-x}$Se$_x$ alloys, respectively are shown in Fig 1.
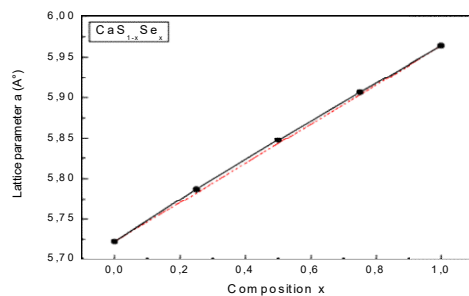

Fig.1. Composition dependence of the calculated lattice Constants (solid squares) of CaS$_{1-x}$Se$_x$ alloy compared with Vegard's prediction (dashed line).

A small deviation from Vegard's law (a linear variation of the lattice constant of alloys versus composition x) is clearly visible with an up-

ward bowing parameter equal to -0.01714 Å for CaS$_{1-x}$Se$_x$ alloys obtained by fitting the calculated values with a polynomial function. Fig. 2 shows the bulk modulus as a function of x for CaS$_{1-x}$Se$_x$ alloys respectively. A Similar behavior was observed for the composition dependence of the bulk modulus for all three alloys. Deviations of the bulk modulus from the linear concentration dependence (LCD) with downward bowing equal to 0.05029 GPa for CaS$_{1-x}$Se$_x$, alloys, was observed. The large value of the bulk modulus bowing for CaS$_{1-x}$Te$_x$ alloy compared to those and for CaSe$_{1-x}$Te$_x$ and CaS$_{1-x}$Se$_x$, is also because of the significant mismatch of the bulk modulus of CaS and CaTe compounds.
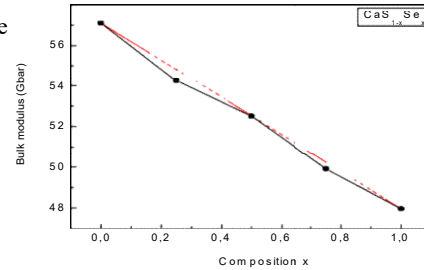

Fig.2. Composition dependence of the calculated bulk modulus (solid squares) of CaS$_{1-x}$Se$_x$ alloy compared with LCD prediction (dashed line).

B. OPTICAL BOWING AND ITS ORIGINS

The self-consistent scalar relativistic indirect band gap of CaX compounds and their alloys was calculated within the GGA and EVGGA schemes. The results for each compound are given in table 2. It is well known that the GGA usually underestimates the energy gap [19-22]. This is mainly due to the fact that the functional within this approximation have simple forms that are not sufficiently flexible to reproduce accurately both exchange correlation energy and its charge derivative. Engel and Vosko by considering this shortcoming constructed a new functional form of the GGA which is able to better reproduce exchange potential at the expense of less agreement in exchange energy. This approach (EVGGA) yields a better band splitting and some other properties which mainly depend on the accuracy of exchange-correlation potential. However, in this method, the quantities that depend on an accurate description of exchange energy E_x such as equilibrium volumes and bulk modulus are in poor agreement with experiment. Therefore we always apply EVGGA to the electronic properties and GGA for the structural properties [20 - 22].

Tableau 2. Band gap energy of CaS$_{1-x}$Se$_x$ alloys at different concentrations (all values are given in eV)

	x	E_g (eV)			
		Our work		Other work	
		GGA	EVGG	GGA[24]	EGGA[24]
CaS$_{1-x}$Se$_x$	1	2.105	2.815	2.10	2.81
	0.75	2.171	2.906		
	0.50	2.235	2.977		
	0.25	2.321	3.089		
	0	2.405	3.176	2.39	3.18

We calculated gap bowing, using the GGA and EVGGA schemes, by fitting the non-linear variation of the calculated band gaps versus concentration with quadratic functions. The results are shown in Fig 3 and obey the following variations

$$CaS_{1-x}Se_x \Rightarrow \quad \begin{array}{l} E_g^{GGA} = 2.406 - 0.366x + 0.066x^2 \\ E_g^{EVGGA} = 3.178 - 0.399x + 0.038x^2 \end{array} \quad (1)$$

The results of the calculated gap bowing are given in table 3. It is clearly seen that the calculated quadratic parameters (gap bowing) within GGA and EVGGA are very close to the results obtained by the Zunger approach. The optical bowing of $CaS_{1-x}Se_x$ alloy was found to be small. In order to better understand the physical origins of the gap bowing in calcium chalcogenides alloys, we follow the procedure of Bernard and Zunger [23] and decompose the bowing parameter (b) into physically distinct contributions.

Fig.3. Composition dependence of the calculated band gap using GGA (solid squares) and EVGGA (solid circles) for $CaS_{1-x}Se_x$ alloy
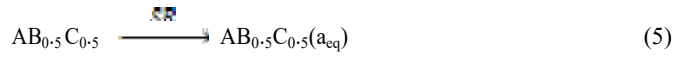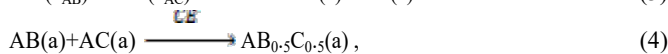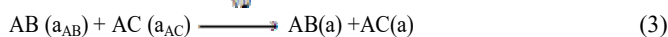
Table 3. Decomposition of the optical bowing into volume deformation (VD), charge exchange (CE), and structural relaxation (SR) contributions compared with the optical bowing obtained by fitting the non-linear variation of the calculated band gap versus concentration with quadratic functions at molar fractions 0.25, 0.50 and 0.75 (all values are given in eV)

parameter	calculation		Quadratic fits	
	GGA	EVGGA	GGA	EVGGA
$CaS_{1-x}Se_x$ b_{VD}	0.052	0.100		
b_{CE}	0.068	0.002		
b_{SR}	-0.040	-0.028		
b	0.080	0.074	0.065	0.036

By considering the fact that the bowing dependence to the composition is marginal, the authors limited their calculations to x=0.5 (50%-50% alloy). The overall gap bowing coefficient at x = 0.5 measures the change in band gap according to the reaction:

$$AB(a_{AB}) + AC(a_{AC}) \rightarrow AB_{0.5}C_{0.5}(a_{eq}) \quad (2)$$
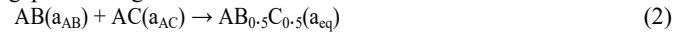
where a_{AB} and a_{Ac} are the equilibrium lattice constants of the binary compounds AB and AC, respectively, and a_{eq} is the alloy equilibrium lattice constant. We now decompose reaction (1) into three steps:

$$AB\ (a_{AB}) + AC\ (a_{AC}) \xrightarrow{\ VD\ } AB(a) + AC(a) \quad (3)$$

$$AB(a) + AC(a) \xrightarrow{\ CE\ } AB_{0.5}C_{0.5}(a), \quad (4)$$

$$AB_{0.5}C_{0.5} \xrightarrow{\ SR\ } AB_{0.5}C_{0.5}(a_{eq}) \quad (5)$$

the total gap bowing parameter b_{VD} represents the relative response of the band structure of the binary compounds AB and AC to hydrostatic pressure, which here arises from the change of their individual equilibrium lattice constants to the alloy value a=a(x) (from Vegard's rule). The second contribution, the charge-exchange (CE) contribution b_{CE}, reflects a charge transfer effect which is due to the different (averaged) bonding behavior at the lattice constant a. The final step measures changes due to the structural relaxation (SR) in passing from the unrelaxed to the relaxed alloy by b_{SR}. Consequently, the total gap bowing parameter is defined as where ϵ is the energy gap which have been calculated for the indicated atomic structures and lattice constants. All term in Eqs. (5) - (8) are calculated separately via self-consistent band structure calculations within density functional theory and the results are given in table 3.

$$b = b_{VD} + b_{CE} + b_{SR}, \quad (6)$$

$$b_{VD} = 2[\varepsilon_{AB}(a_{AB}) - \varepsilon_{AB}(a) + \varepsilon_{Ac}(a_{Ac}) - \varepsilon_{Ac}(a)], \quad (7)$$

$$b_{CE} = 2[\varepsilon_{AB}(a) + \varepsilon_{AC}(a) - 2\varepsilon_{ABC}(a)] \quad (8)$$

$$b_{SR} = 4[\varepsilon_{ABC}(a) - \varepsilon_{ABC}(a_{eq})] \quad (9)$$

The total gap bowing is found to be small for the $CaS_{1-x}Se_x$ alloy, while for the two other corresponding alloy. The contribution of the volume deformation term to the bowing parameter b_{VD} has been found to be significant for $CaS_{1-x}Se_x$. This term is correlated to the mismatch of the lattice constants of the corresponding binary compounds. The charge transfer contribution b_{CE} has been found smaller than b_{VD} but it is not negligible for $CaS_{1-x}Se_x$. this contribution is due to the large electronegativity difference between S and Se atoms. Indeed, the significant role of b_{CE} is correlated with iconicity factor difference between constituent binary compounds CaS (fi=0.43) and CaSe (fi=0.38).

C. THERMODYNAMIC PROPERTIES

Focusing on the thermodynamic properties of $CaS_{1-x}Se_x$ alloys, we calculated the phase diagram based on the regular-solution model [25-27]. The Gibbs free energy of mixing, ΔG_m for alloys is expressed as

$$\Delta G_m = \Delta H_m - T\Delta S_m \quad (10)$$

Where:

$$\Delta H_m = \Omega\, x\,(1-x), \quad (11)$$

$$\Delta S_m = -R[x \ln x + (1-x)\ln(1-x)]. \quad (12)$$

ΔH_m and ΔS_m are the enthalpy and entropy of mixing, respectively; Ω the interaction parameter, R is the gas constant and T is the absolute temperature. Only the interaction parameter Ω depends on the material.

The mixing enthalpy of alloys can be obtained from the calculated total energies as $\Delta H_m = E_{ABxC1-x} - xE_{AB} - (1-x) E_{Ac}$, where $E_{ABxC1-x}$, E_{AB}, and E_{AC} are the respective energies of AB_xC_{1-x} alloy and the binary compounds AB and Ac. We then calculated ΔH_m to obtain Ω as a function of concentration.. The interaction parameter increases almost linearly with increasing x. From a linear fit we obtained

$$CaS_{1-x}Se_x \implies \Omega\ (Kcal/mol) = -0.324x + 1.580x \quad (13)$$

The average values of the x-dependent Ω in the range $0 \le x \le 1$ obtained from these equations for $CaS_{1-x}Se_x$ alloys is 1.418 (Kcalmol^{-1}) respectively. The large enthalpy for $CaS_{1-x}Te_x$ alloy suggest a large value of Ω and hence a higher critical temperature.

We calculated the temperature-composition phase diagram which shows the stable, metastable and unstable mixing regions of the alloy. At a temperature lower than the critical temperature T_c, the two bimodal points
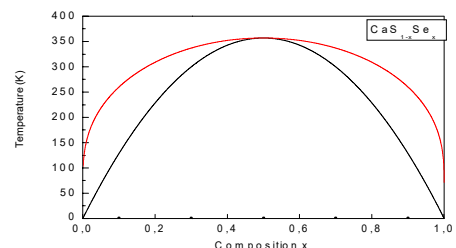
are determined as those points at which the common tangent line touches the ΔG_m curves. The two spinodal points are determined as those points at which the second derivative ΔG_m is zero. Fig. 5 displays the calculated phase diagrams including the spinodal and binodal curves of alloys of interest. We observed a critical temperature T_c of 357.8 for $CaS_{1-x}Se_x$ alloys, respectively. The spinodal curve in the phase diagram marks the equilibrium solubility limit, i.e., the miscibility gap. For temperatures and compositions above this curve a homogeneous alloy is predicted. The wide range between spinodal and binodal curves indicates that the alloy may exist as metastable phase.

Fig.4. T-x phase diagram of $CaS_{1-x}Se_x$ alloy. Dashed line: bimodal curve; solid line: spinodal curve.

D. OPTICAL PROPERTIES

In this section we analyze the most important measurable quantity is the dielectric function of the system which is a complex quantity given by

$$\varepsilon(\omega) = \varepsilon_1(\omega) + i\varepsilon_2(\omega)$$

Where $\varepsilon_1(\omega)$ and $\varepsilon_2(\omega)$ represent the real and the imaginary parts of the dielectric function. the imaginary parts of $\varepsilon_2(\omega)$, depends on the joint density of state and the momentum matrix elements. The real part of the dielectric function, $\varepsilon_1(\omega)$, was obtained from by the Kramers-Kronig realations. The properties optic ofthe semiconductor alloys are important and essential in the design and fabrication of devices. In the design and analysis these devices, the refractive index and optical dielectric constants of the material of interest have to be known as a function of composition and wavelength. In this theoretical work, we calculated the refractive index and the optical dielectric constant and compared with different models. $n(\omega)$ is given by expression (14).

$$n(\omega) = \frac{\varepsilon_1(\omega)}{2} + \frac{\sqrt{\varepsilon_1^2(\omega) + \varepsilon_2^2(\omega)}}{2}^{1/2} \quad (14)$$

At low frequency ($\omega=0$), we get the following relation

$$n(0) = \varepsilon^{1/2}(0) \quad (15)$$

1. The Moss formula [28] based on an atomic model.

$$E_g n^4 = k \quad (16)$$

Where E_g is the energy band gap and ka constant. The value of k is given to be 108 eV by Ravindra and Srivastava [28]

2. The expression proposed by Ravindra and all [29].

$$n = \alpha + \beta_{E_g} \quad (17)$$

With $\alpha = 4.084$ and $\beta = -0.62$ eV^{-1}

3. Herve and Vandamme's empirical relation [30]

$$n = \sqrt{1 + \left(\frac{A}{E_g + B}\right)^2} \quad (18)$$

With $A = 13.6$ eV and $B = 3.4$ eV

The variation of the refractive index for the three alloys of interest as a function the concentration x has been studied. Our results are plotted in fig6

{(a)-(c)}. Through Fig 6, one can notice that the refractive index increases monotonically with increasing concentration x content over the entire of 0-1 for all models used. However, it does not behave in a similar fashion on going from one model to another one. This is clearly seen from the following quadratic polynomial fit to these data for the three alloys:

$$CaS_{1-x}Se_x \Rightarrow \begin{cases} n_1(x) = 2.581 + 0.111\ x - 0.023\ x^2 \\ n_2(x) = 2.590 + 0.214\ x - 0.034\ x^2 \\ n_3(x) = 2.539 + 0.143\ x - 0.023\ x^2 \\ n_4(x) = 2.290 + 0.026\ x + 0.002\ x^2 \end{cases}$$

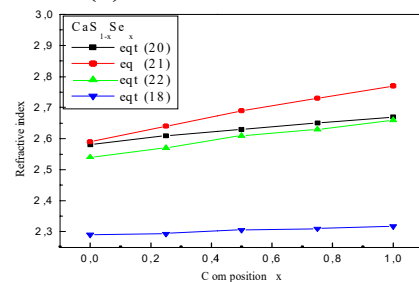**Fig.5.** Refractive index of the of $CaS_{1-x}Se_x$ alloys for different compositions x

E. CONCLUSION

In summary, we have studied the structural, electronic, optic and thermodynamic properties of $CaS_{1-x}Se_x$ alloys by using the FP-LAPW method. We have optimized the lattice parameter for binary compounds as well as for alloys. The lattice constant of $CaS_{1-x}Se_x$ alloys exhibits a small deviation from Vegar's law with bowing parameters is equal to -0.00437 Å. The investigation of the thermodynamic stability allowed us to calculate the critical temperatures for $CaS_{1-x}Se_x$ alloys, which is 357.8. Finally we have reported the optoelectronic properties of ternary alloys. The calculated refractive index and optical dielectric constants for the parent compounds show better agreement with the known data. Compositional dependence of the optical and electronic properties studied is also investigated.

REFERENCES

[1] Pandey R, Sivaraman S 1991 *J. Phys. Chem. Solids* **52** 211
[2] Asano S, Yamashita N, Nakao Y 1978 *Phys. Status. Solidi* **89** 663
[3] Nakanishi, Ito T, Hatanaka Y, Shimaoka G 1992 *Appl. Surf. Sci* **66** 515
[4] Zunger A, Wei S H, Ferreira L G and Bernard J E 1990 *Phys. Rev. Lett* **65** 353
[5] Koelling D D and Harmon B N 1977 J. Phys. C: Solid State Phys. **10** 3107
[6] Blaha P, Schwarz K, Madsen G K H, Kvasnicka D and Luitz J 2001 WIEN2K, *An Augmented Plane Wave+Local Orbitals Program for Calculating Crystal Properties* Karlheinz, Techn. Universitat, Wien, Austria (ISBN 3-9501031-1-2)
[7] Kohn W and Sham L J 1965 *Phys. Rev.* A **140** 1133
[8] Perdew J P, Burke S and Ernzerhof M 1996 *Phys. Rev. Lett.* **77** 3865
[9] Engel and Vosko S H 1993 *Phys. Rev.* B **47** 13164
[10] Murnaghan F D 1944 *Proc. Natl Acad. Sci. USA* **30** 244
[11] Chrifi Z, Baaziz H, El Haj Hassan and Bouarissa N (2005) *J. Phys. Condens. Matter* **17** 4083
[12] Vegard L 1921 *Z. Phys*. **5** 17

[13] Jobst B, Hommel D, Lunz U, Gerhard T and Landwehr G 1996 *Appl. Phys. Lett.* **69** 97

[14] Dismuckes J P, Ekstrom L and Poff R J 1964 *J. Phys. Chem.* **68** 3021

[15] El Haj Hassan F and Akdarzadeh H 2005 *Mater. Sci. Eng.* B **121** 170

[16] El Haj Hassan F 2005 *Phys. Status Solidi* b **242** 909

[17] Luo H, Greene R G, Handechari K G, Li T and Ruoff A L 1994 *Phys. Rev.* B **50** 16232

[18] Cortona P and Masri P 1998 *J. Phys. Condens. Matter* **10** 8947

[19] Martins J L and Zunger A 1986 *Phys. Rev. Lett.* **56** 1400

[20] Dufek P, Blaha P and Schwarz K 1994 *Phys. Rev.* B **50** 7279

[21] El Haj Hassan F, Akdarzadeh H and Hashemifar S J 2004 *J. Phys. Chem. Solids* **16** 3329

[22] El Haj Hassan F, Akdarzadeh H, Hashemifar S J and Mokhatari A 2004 *J. Phys. Chem. Solids* **65** 1871

[23] Srivastava G P, Martins G L and Zunger A 1985 *Phys. Rev.* B **31** 2561

[24] Charifi Z, Baaziz H, El Haj Hassan F and Bouarissa 2005 *J. Phys. Condens. Matter* **17** 4083-4092

[25] Swalin R A, Thermodynamics of solids (John Wiley, New York, 1961)

[26] Ferreira L G, Wei S H, Bernard J E and Zunger A 1989 *Phys. Rev.* B **40** 3197

[27] Teles L K, Furthmüller, Scolfaro, Leite and Bechstedt F 2000 *Phys. Rev.* B **62** 2475

[28] Gupta V P, Ravindra N M *Phys. Stat. Solid* (b) 100 (1980) 715

[29] Ravindra N M, Auluck S, Srivastava V K, Phys. Stat. Solid. (b) 93 (1979) k155

[30] Herve P J L, Vandamme L k J, *Infrared Phys. Technol.* 35 (1994) 609.